2014-05

Modulation of Contact Resistance between Metal and Graphene by Controlling the Graphene Edge, Contact Area, and Point Defects: An Ab Initio Study

UTD AUTHOR(S): Cheng Gong and Kyeongiae Cho

AIP | Journal of Applied Physics

Modulation of contact resistance between metal and graphene by controlling the graphene edge, contact area, and point defects: An ab initio study

Bo Ma, Cheng Gong, Yanwei Wen, Rong Chen, Kyeongjae Cho, and Bin Shan

Citation: Journal of Applied Physics **115**, 183708 (2014); doi: 10.1063/1.4876738
View online: http://dx.doi.org/10.1063/1.4876738
View Table of Contents: http://scitation.aip.org/content/aip/journal/jap/115/18?ver=pdfcov
Published by the AIP Publishing

JOURNAL OF APPLIED PHYSICS **115**, 183708 (2014)

Modulation of contact resistance between metal and graphene by controlling the graphene edge, contact area, and point defects: An *ab initio* study

Bo Ma,[1] Cheng Gong,[2] Yanwei Wen,[1,a)] Rong Chen,[3] Kyeongjae Cho,[2] and Bin Shan[1,2,a)]
[1]*State Key Laboratory of Material Processing and Die and Mould Technology and School of Materials Science and Engineering, Huazhong University of Science and Technology, Wuhan, Hubei 430074, People's Republic of China*
[2]*Department of Materials Science and Engineering, The University of Texas at Dallas, Richardson, Texas 75080, USA*
[3]*State Key Laboratory of Digital Manufacturing Equipment and Technology and School of Mechanical Science and Engineering, Huazhong University of Science and Technology, Wuhan, Hubei 430074, People's Republic of China*

(Received 28 November 2013; accepted 4 May 2014; published online 14 May 2014)

A systematic first-principles non-equilibrium Green's function study is conducted on the contact resistance between a series of metals (Au, Ag, Pt, Cu, Ni, and Pd) and graphene in the side contact geometry. Different factors such as the termination of the graphene edge, contact area, and point defect in contacted graphene are investigated. Notable differences are observed in structural configurations and electronic transport characteristics of these metal-graphene contacts, depending on the metal species and aforementioned influencing factors. It is found that the enhanced chemical reactivity of the graphene due to dangling bonds from either the unsaturated graphene edge or point defects strengthens the metal-graphene bonding, leading to a considerable contact resistance reduction for weakly interacting metals Au and Ag. For stronger interacting metals Pt and Cu, a slightly reduced contact resistance is found due to such influencing factors. However, the wetting metals Ni and Pd most strongly hybridize with graphene, exhibiting negligible dependence on the above influencing factors. This study provides guidance for the optimization of metal-graphene contacts at an atomic scale. © *2014 AIP Publishing LLC*. [http://dx.doi.org/10.1063/1.4876738]

I. INTRODUCTION

Graphene is a promising material that has wide potential use in future nano-electronics due to its superior electronic properties and the atomic thickness.[1–4] In graphene-based nanodevices, metal-graphene (M-G) contact is one of the critical factors that determine the device performance such as transconductance (g_m), on-current (Ion), and cut-off frequency (f_T). Thus, a fundamental understanding of the interfacial electron transport behaviors between metal and graphene is a key step toward the rational design and fabrication of graphene-based devices.

For the model system where an infinite graphene monolayer is adsorbed on metal surfaces, some theoretical studies suggest that strongly interacting metal electrodes show less contact resistance than those weakly interacting ones.[5–8] However, experimentally reported contact resistances (R_C), extracted based on either transfer length measurement (TLM) or a four-probe method, show considerable device-to-device variation.[9–15] In these experiments, weakly interacting metals, such as Au, Ag, and Cu, have also been shown to have low Rc,[9,10,15,16] even in the side contact geometry. One possible reason for such discrepancy is that the effects caused by graphene terminations, contacts area, defects, etc., in realistic experiments have been overlooked in idealized theoretical models. Recently, Stokbro *et al.* and Liu *et al.* independently studied the relationship between atomistic details and transport properties of nickel and graphene. Stokbro's work showed that Ni-G contact is insensitive to the termination of graphene edge and contact area.[17] However, Liu *et al.* concluded that Ni-G contact resistance decreases with the increase of contact area at low bias voltage.[18] Although it is known that Ni is strongly interacting with graphene in contact, the effect of contact area on the transport properties of the Ni-G contact is still in controversy. As indicated by a previous study, the defects in graphene could greatly enhance the interaction between metal and graphene,[19] the transport properties of M-G contact is also expected to change a lot due to the introduction of defect. Other factors such as chemical activity of graphene, subject to the impact of the specific experimental process, may also play an important role in the real contact resistance. How these detailed atomistic configurations in real graphene devices affect the contact resistance of both weakly and strongly interacting M-G remains unclear. Clarifying the impact of these factors on the transport properties can not only help understand the interaction at M-G contacts but also be of significant interest to advance the graphene electronic devices.

In this Letter, we report a systematic investigation of the effects of different factors, including graphene edge termination, contact area, and point defects in the contact region, on transport properties of the side contact geometry between six representative metal electrodes (Au, Ag, Pt, Cu, Ni, and Pd) and graphene. It is found that the dependence of contact

a)Authors to whom correspondence should be addressed. Electronic addresses: ywwen@hust.edu.cn and bshan@mail.hust.edu.cn.

resistance on these factors can be categorized into three types according to their bonding strengths. Those metal electrodes that interact only weakly with graphene such as Au and Ag are very sensitive to the detailed atomistic configurations at the contact region. For these weakly interacting metals, open graphene edges without chemical terminations, small contact length, and point defects could introduce chemical bonds at the contact region, resulting in the decreased contact resistance. In sharp contrast, the contact resistances between graphene and strongly interacting metals, such as Ni and Pd, show little sensitivity to these factors. Pt and Cu, as an intermediate type of metals, show a slight dependence on the influencing factors in contact with graphene. Potential-drop contours, π electron local density of states (LDOS), and bond current analysis were performed to elucidate the difference of these three types of contact. The results hint that weakly interacting metals likely form low contact resistance with graphene by engineering the chemical reactivity of the part of the contacted graphene.

II. METHODOLOGY

In a number of previous transport calculations, a semi-infinite metal-graphene complex is treated as electrodes.[20–22] While the model is of scientific interest, such configuration may not yield a realistic picture of the charge injection from the metal into graphene. Hence, we adopt a side contact model in which the left electrode consists only of metal atoms.[8] Such configuration counts the carrier injection from metal electrodes to the graphene channel and the effect of the graphene edge. The orientation of the graphene edge is chosen to be zigzag as it is energetically more stable.[23] We considered open-ended or hydrogen-terminated graphene edges (Fig. 1(a)) as both terminations are possible depending on the etching process.[24,25] Metals are taken as the left electrode and the suspended graphene sheet is used as the right electrode as shown in Fig. 1(b). The length of the overlapping contact between graphene and metal surface is initially fixed to the same lengths (~8 Å) for comparison among different metal species and various graphene edges. Subsequently, we vary the contact length from 4 Å to 16 Å to investigate the effect of contact area on the contact configuration and resistance. Finally, point defects are introduced into the graphene of contact region to investigate the effect of defects.

The lattice constants of all the studied metals are slightly strained to match graphene, as shown in Figs. 1(c) and 1(d). The optimization of M-G contact geometry is performed under local density approximation as implemented in the Vienna *ab initio* simulation package (VASP).[26] After getting the optimal contact configurations, the electronic transport properties are calculated using *ab initio* non-equilibrium Green's function code (NEGF) TranSiesta.[27,28] 150 Ry mesh cut off and single-zeta plus polarization basis (SZP) are used in our self-consistent calculations, which have been proven sufficient in the studied systems.[29,30] The transmission and current are calculated with 251 k-points for Au(Ag, Pt, and Pd) and 501 k-points for Ni(Cu) in the periodical direction(x-direction). The length of the unit cell of the semi-infinite electrode in z-direction is 8.52 Å, and 101 k-points are used in z-direction to generate the surface Green's function and reproduce the semi-infinite electrodes, and the convergence of the number of K-points in the calculations has been tested.

III. RESULTS AND DISCUSSION

A. Graphene edge

The different terminations of the graphene edge are first considered for the common existence in graphene electronic devices. Two distances d_1 and d_2 are used to characterize the equilibrium geometry of the M-G contact at different positions of the contacts as shown in Fig. 1(b). Table I summarizes the equilibrium distances, including the one (di) for ideal metal-graphene side contact for comparison.[31] It is found that the studied metal species can be classified into three types for contacting the graphene end. Noble metals Au and Ag can form strong chemical bonds only with the

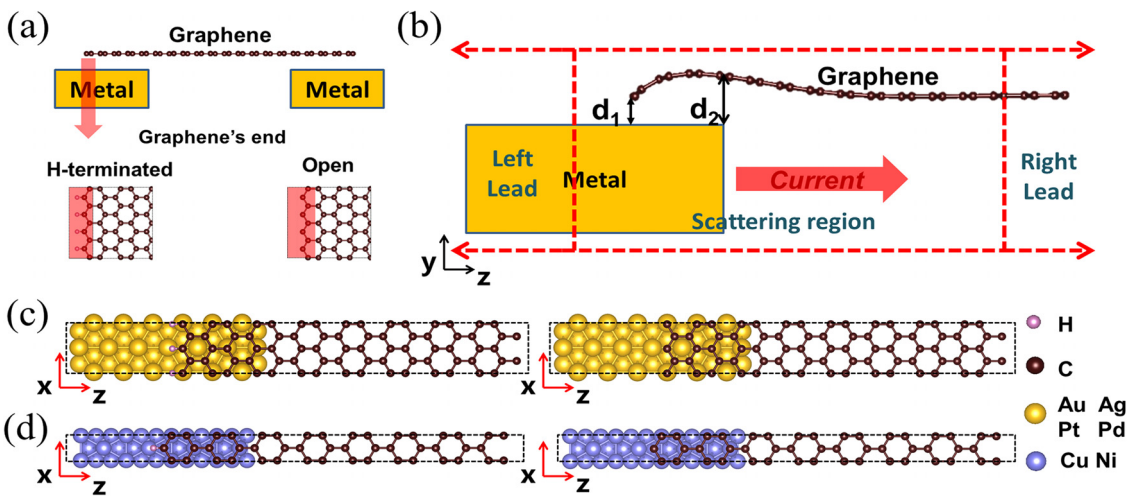

FIG. 1. (a) Schematics of a graphene field effect transistor and the open and H-terminated graphene ends. (b) The side-view of the transport calculation model of the contact between metal (111) surface and graphene with an open zigzag end. (c) Top views of models of graphene on the Au (111), Ag (111), Pt (111), and Pd(111) surfaces and (d) Ni (111) and Cu(111) surfaces with H-terminated and open zigzag end.

TABLE I. Equilibrium distances for the infinite M-G side contact and M-G side contact at graphene zigzag edge with H-terminated and open graphene end.

	H-terminated		Open		Bulk
	d_1 (Å)	d_2 (Å)	d_1 (Å)	d_2 (Å)	d_i (Å)
Au	3.02	3.28	2.00	3.62	3.51
Ag	2.67	2.93	2.02	3.33	3.30
Cu	2.18	2.64	1.94	2.80	2.98
Pt	2.16	3.04	1.86	3.72	3.25
Pd	2.12	2.12	1.85	2.17	2.41
Ni	1.94	1.98	1.65	2.04	2.04

open graphene ends and interact with graphene weakly at other regions. Pt and Cu belong to the second category that interacts strongly with both open and hydrogen terminated ends, while keeps weak bonding away from ends. The third type of metals (Pd and Ni) form chemical bonds throughout the whole contact region with all types of graphene ends. This classification is slightly different from the metal classification when interacting with an infinite graphene layer, where metals are generally divided into two types: strongly and weakly interacting metals.[31,32] This difference is due to the fact that graphene ends (both open-ended and hydrogen terminated) have higher reactivity than the pristine graphene surface and can bond with some weakly interacting metals more effectively. It is worthwhile noting that the hydrogen-passivated zigzag end is able to form chemical bonds with Pt and Cu, indicating higher reactivity of graphene ends than the pristine graphene surface (see Fig. S1 in supplementary material[39]). These observations indicate the type of graphene end is as important as the metal species in determining the detailed contact configurations, which would affect the charge transport properties of the M-G contacts essentially.

To figure out the effects of the graphene end on the transport properties of M-G side contact, we calculate the transmission spectra and I-V curves. We show the transmission spectra and I-V curves of three representative M(Au, Pt, and Pd)-G contacts in Fig. 2. We first discuss the strongly interacting metals using Pd as an example for it is one of the most widely used metal electrodes in experiments. It can be seen that the transmission coefficients near the Fermi level and the current under specific voltage for Pd-G contacts with both open and H-terminated ends are similar to each other and are higher than the other metal-G contacts. It shows that the Pd-G and Pt-G are obviously superior to the Au-G contact and the graphene ends have little effect on the transport properties of these two contacts. The result is consistent with the previous theoretical study of Ni contact, which is also a strongly interacting metal.[17] In contrast, the chemistry of graphene ends in Au-G side contact affects the transport properties significantly. The current of Au contact to open-ended graphene is 3.40 μA, about four times larger than that of H-terminated graphene (0.78 μA) under a 0.6 V bias voltage. The transmission coefficient for Au-G contact with open end is obviously higher than the H-terminated one. Pt, which weakly interacts with infinite graphene sheet in side contact geometry,[31,32] forms an effective contact with both the open and hydrogen terminated ends, exhibiting transmission and I-V curves as from strongly interacting metal-graphene contacts. This observation indicates that both graphene ends are chemically reactive, leading to reduced contact resistance. These results suggest alternative ways of reducing contact resistance of weakly interacting metal-graphene contacts, by engineering the graphene ends. Interestingly, recent experiments demonstrated that the

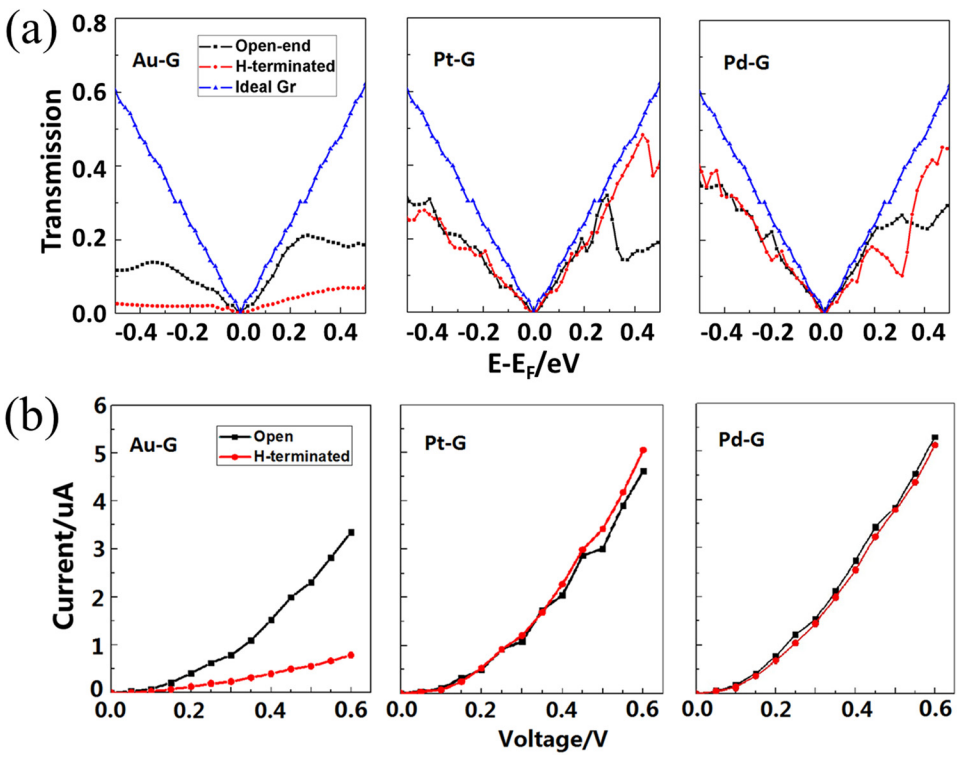

FIG. 2. (a) Transmission spectra and (b) I-V curves for Au-G, Pt-G, and Pd-G contacts with different ends.

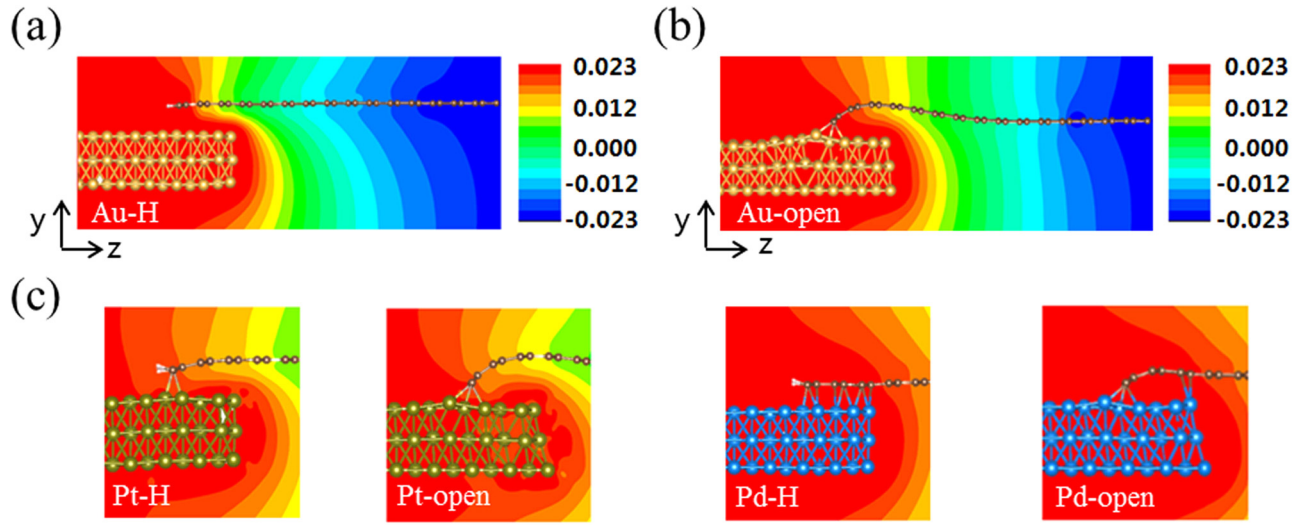

FIG. 3. Potential-drop contours for the whole Au-G side contact with (a) H-terminated graphene end and (b) open graphene end at 0.6 V bias, (c) potential-drop contours in local contact region for Pt-G and Pd-G with H terminated and open ends at 0.6 V bias.

enhanced carrier injection and lower contact resistance can be achieved by forming cuts in the graphene within the contact region to maximize the "edge-contacted" injection.[33] Our simulation results provide insightful understanding on these experimental observations.

To gain further insight into the microscopic details on the origin of the contact resistance, we plot the potential drop at 0.60 V bias for these contacts with graphene ends in Fig. 3. The average potential drop along the transport direction (z-direction) shows quite different characteristics and its gradient is an indicative of the contact resistance. Figure 3(a) shows the potential-drop of Au-G with a H-terminated end, and it is found that the potential drops sharply in the contact region, indicating a potential barrier and a large electronic resistance in this local region.[34] Figure 3(b) shows the potential-drop contour for Au-G with an open end for comparison, and we note that the potential drop is more smooth and gradual, which is a reflection of lower resistance due to the bond formation between Au and the terminal carbon atoms on the graphene end. It provides an insight that by reactive etching, the promotion of metal-carbon bonds formation can effectively decrease the contact resistance for Au-G side contact. For Pd-G or Pt-G side contacts, the potential-drops with both open and H-terminated ends are similar in the contact regions, as shown in Figs. 3(b) and 3(c). We note that the potential drops most smoothly at Pd-G contact among the three studied M-G contacts, which agrees with the calculated I-V curves where Pd-G contact shows the smallest contact resistance.

Among the M-G contacts with H-terminated graphene ends, the resistance of Au-G is much higher than that of Pd-G. To understand the notable difference, we plot the π electrons' LDOS of each carbon atoms along the graphene channel for both contacts under equilibrium conditions, as shown in Figs. 4(b) and 4(c). The carbon atoms close to the graphene edge are numbered from left to right (Fig. 4(a)), and the color bar represents the magnitude of DOS of each carbon atoms near the Fermi level. As shown in Fig. 4(b), spatially disconnected density of states is observed. It would enhance the electron scattering greatly and thus increase the resistance of Au-G contact, consistent with the I-V characteristic and potential-drop plot. In contrast, the LDOS of Pd-G contact in Fig. 4(c) is more uniform. It is reasonable because Pd forms strong bonds with graphene in the whole contact region and the Pd-C hybridization offers transport channels for electrons. The hybridization effect extends several angstroms into the suspended graphene channel and thus promises the larger conductance.

To determine the resistance and charge injection at the atomic level, the bond-current between each two atoms is calculated by the Inelastica, the post-processing package for Transiesta at the Fermi energy ($(\mu_L + \mu_R)/2$) within a small bias voltage.[35–37] We sum the percentage of the current flow from each metal surface atom to graphene for Au-G and Pd-G side contacts, shown in Figs. 4(d) and 4(e). For the Au-G contact, the current injection mainly takes place at the very end of graphene due to the localized π electrons density of states at the graphene end, while the current injection occurs in the whole Pd-G contact because of the uniform π electrons density of states. Combined with the LDOS analysis, the fluctuated LDOS of Au-G contact with the H-terminated end would seriously hinder the current flow in graphene edge and yield a large contact resistance. Though the bond current injection of Pd-G contact extends the whole contact region, there is a large percent of current flow back from graphene layer to the 4th Pd surface atoms. The current from 6th Pd surface atom (the end of the metal slab) to graphene mainly contributes to the net current. This observation explains why Pd-G contact shows a negligible potential drop in the contact region and the contact resistance between strongly interacting metals and graphene is insensitive to the contact length.

B. Contact area

The interfacial interaction is not only strongly dependent on metal species and the chemistry of the graphene end but also on the contact area, another key factor of the contact

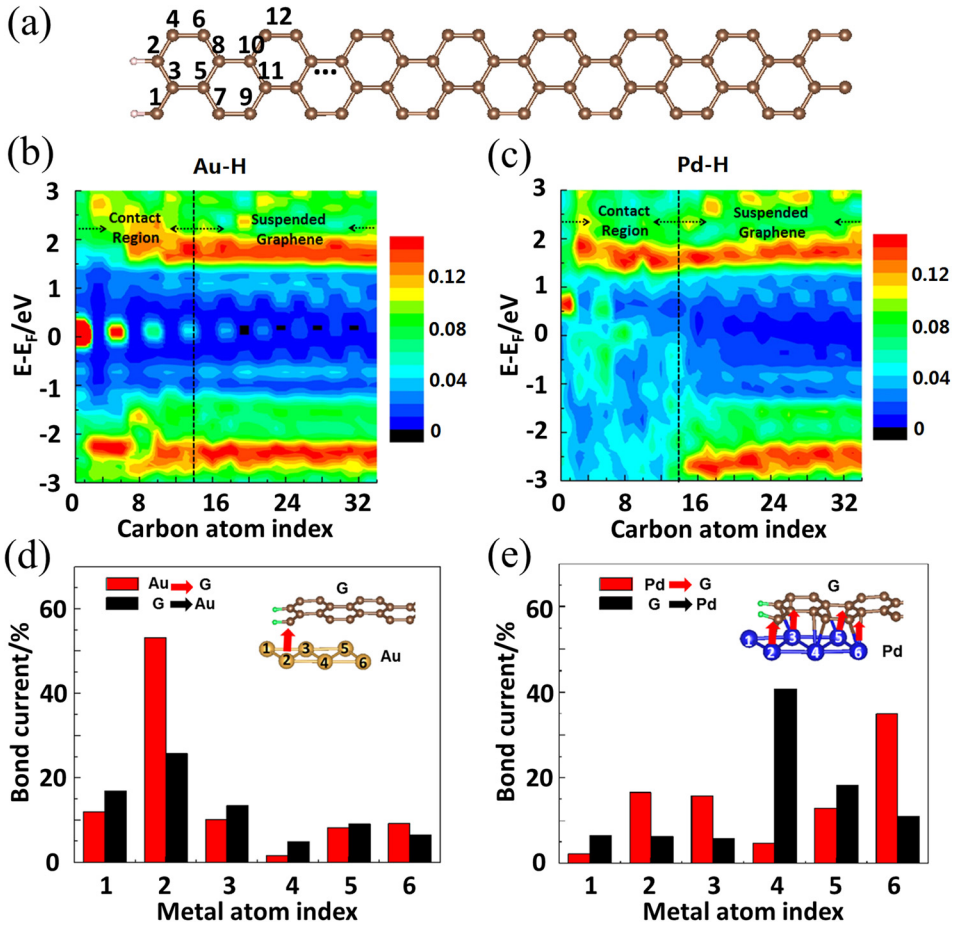

FIG. 4. (a) The carbon atom index in H-terminated graphene channel. π-orbital LDOS contours along the graphene channel for (b) Au-G and (c) Pd-G side contacts with H-terminated end. (d) and (e) are the percentages of current flow from each metal surface atoms to graphene for Au-G and Pd-G, respectively.

resistance. To study the effect of the contact area on contact resistance, we fix the width of the periodical direction of the contact to be 4.92 Å and vary the contact length from 4 Å to 16 Å, for Au, Pt, and Pd contacting with hydrogen terminated graphene. These three contacts represent three typical types of M-G contacts with the H-terminated graphene end: Au forms physical bonds in the whole contact region, Pt only forms chemical bonds at the graphene end, and Pd forms chemical bonds in the whole contact region.

According to the optimized structures, we find that Pd forms chemical bonds with graphene in the whole contact region for all different contact lengths with ~2.20 Å interface distance. As shown in Figs. 5(a) and 5(b), Au could form chemical bonds at the graphene end only if the contact length decreases to ~4 Å, which is evidenced by the interface distance of d_1 (2.32 Å). While it keeps physical interface distance (d_1,$d_2 > 3$ Å) with graphene for ~8 Å, ~12 Å, and ~16 Å overlapping lengths. The enhanced bonding at the Au-G contact with ~4 Å contact length is due to the higher activity of edge metal atom and edge carbon atoms. Different from Au-G, the chemical bonds are always formed at the graphene end for Pt-G for all the studied contact areas.

The transport properties of the three M-G contacts with different contact lengths are calculated. We note the I-V curves of Pd-G contacts with different contact lengths are almost the same, shown in Fig. 2. It shows little effect of the contact area on strongly interacting M-G contacts, consistent with the Stokbro's findings.[17] While Liu *et al.* concluded the

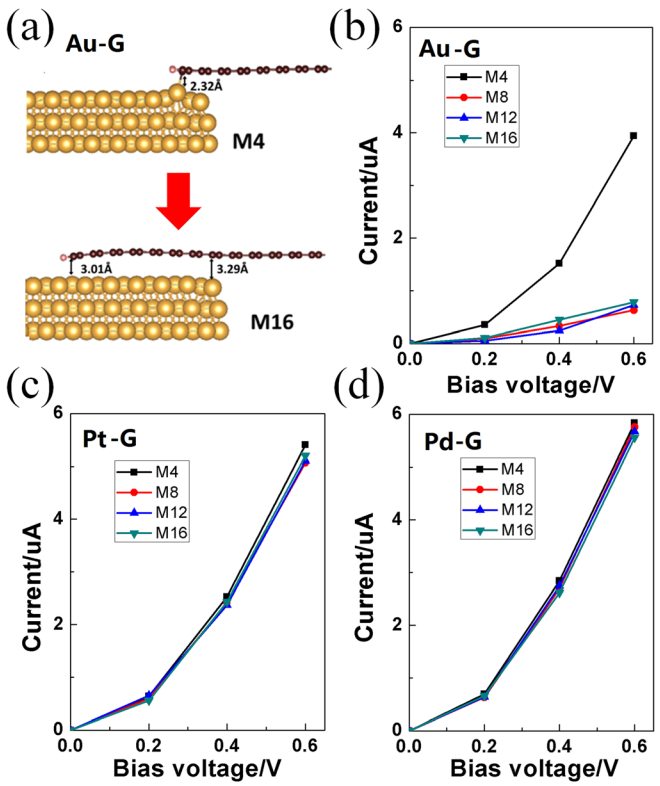

FIG. 5. (a) The side contact between Au and graphene with ~4 Å and ~16 Å contact lengths. I-V curves for (b) Au-G, (c) Pt-G, and (d) Pd-G with different contact lengths.

obvious change of contact resistance with respect to the contact length at low bias voltage. The difference between our results and Liu's conclusion[18] might be attributed to the different calculation models used. Liu's model varies the graphene channel length between two electrodes while changing the contact area, which may affect the contact resistance of the Ni-G. In contrast to Pd-G contact, Fig. 5(b) shows the noticeable effect of contact area on transport properties of Au-G contact. The Au-G contact of ~4 Å contact length shows great enhancement of conductance compared with other contact lengths. Such enhancement is mainly due to the formation of chemical bonds at the graphene end. However, the conductance of Au-G contact shows slight change when the contact length extends over 8 Å. However, the I-V curves in Fig. 5 show that contact area has little effect on the Pt-G contact, similar to the Pd-G contact. This finding suggests that shrinking the contact length to subnanometer scale facilitates the strong metal-carbon bonding for weakly interacting metal-graphene contacts, leading to a reduced contact resistance.

C. Point defects

Sections III A and III B show that chemical bonds between graphene and metals improve the charge injection at M-G contacts. It is therefore expected that defects in graphene may affect the transport properties of M-G contact, particularly when defects exist at the contact region. Hence, it is essential to study the effect of point defects to fully understand the issue of contact resistance in the realistic graphene electronic devices.

We first study the formation energy of a carbon vacancy in M-G contacts, based on the model of a single carbon vacancy in a 14.76 Å × 14.76 Å hexagonal supercell (Fig. 6(a)) for the three typical contacts: Au-G, Pt-G, and Pd-G. With respect to the metal surface, the C vacancy can be at either top site or bridge site, as illustrated in Fig. 6(a). The formation energy of a single C vacancy in the M-G contact is defined as

$$E_f = E(M\text{-}G\_defect) + E(C\_bulk) - E(M\text{-}G\_ideal), \quad (1)$$

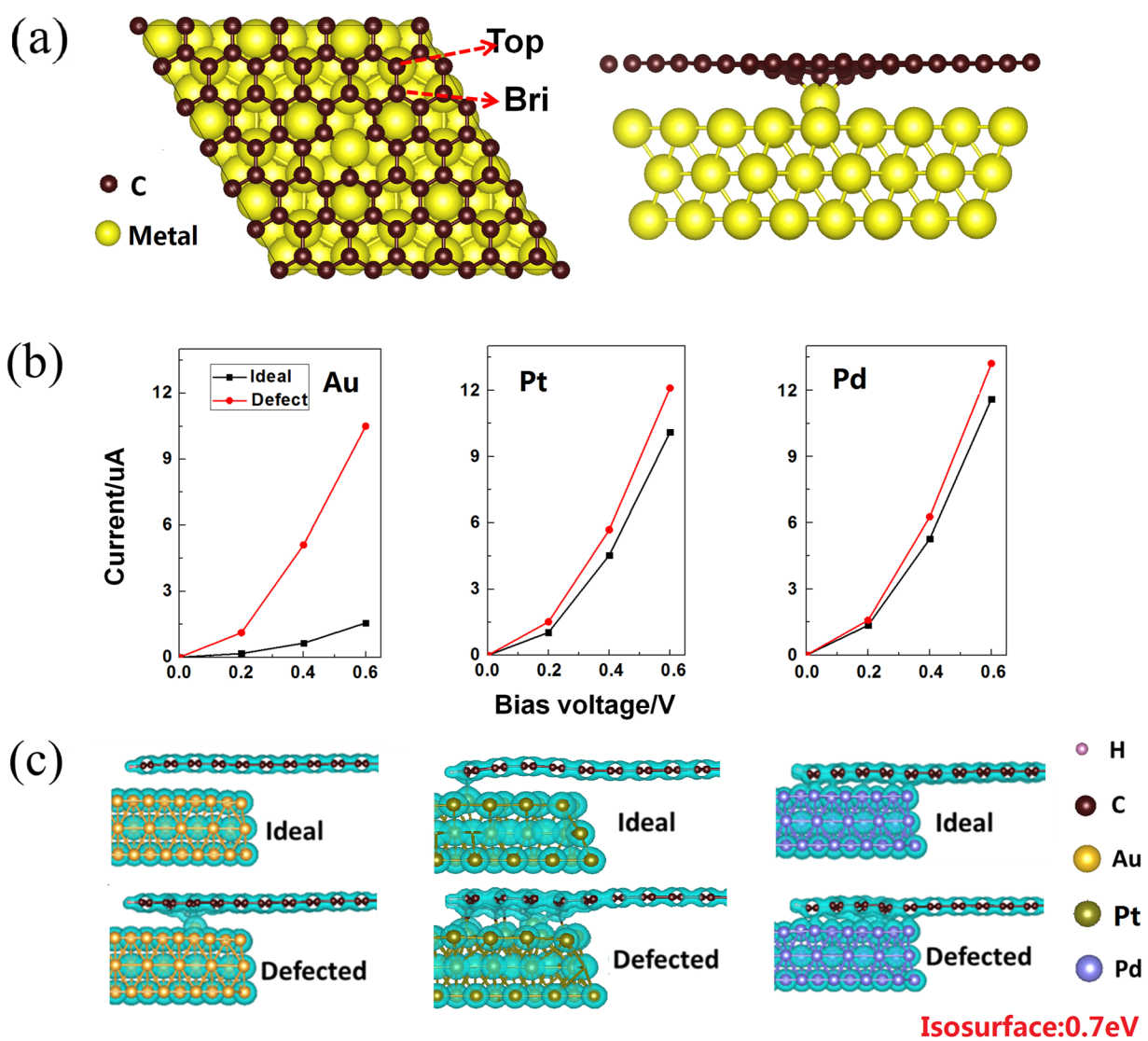

FIG. 6. (a) Top-view and side-view of the side contact with two types of vacancy sites (bridge and top sites). (b) I-V curves for Au-G, Pt-G, and Pd-G contacts with and without point defect in graphene. (c) Electrostatic potential for Au-G, Pt-G, and Pd-G contacts without and with point defects in graphene.

TABLE II. Formation energy of vacancies at different graphene sites in M-G contacts and in pristine graphene.

	Formation energy (eV)	
	Top	Bridge
Au-G	6.81	7.63
Pt-G	2.65	6.24
Pd-G	3.41	5.84
Pristine graphene	8.25	

where the $E(M\text{-}G\_defect)$ and $E(M\text{-}G\_ideal)$ are the total energy of the M-G contact with and without a point defect, $E(C\_bulk)$ denotes the energy of one carbon atom in pristine graphene. Thus, E_f implies the energy needed to create a single C vacancy in the contact. The formation energies of both top and bridge sites are listed in Table II, and the single C vacancy formation energy in pristine graphene is shown for comparison. The calculated single vacancy formation energy in pristine graphene is endothermic with 8.25 eV, in good agreement with a previous study.[38] The formation energies of both top and bridge sites in M-G contact are smaller than that of graphene, which indicates the point defect formation is easier to occur than in pristine graphene. The decreased formation energy may be due to the additional bonding between the defective graphene and the metal. We notice that the formation energy for each site of Au-G is higher than that of Pt-G and Pd-G, which is reasonable since the Au-C bonding is weaker than Pt-C and Pd-C bonding. Moreover, an easier formation of the point defect is found to be at the top site for M-G contact.

To investigate the bonding between the defective graphene and metal slabs, we calculate the binding energy of the two components of the contact, which is defined as

$$E_b = E(M\text{-}G\_defect) + E(G\_defect) - E(M), \qquad (2)$$

where $E(M\text{-}G\_defect)$ is the total energy of M-G contact with defect, $E(G\_defect)$ and $E(M)$ are the total energies of the graphene with defect and the metal slab, respectively. The negative sign of the binding energy means the favored binding between the defective graphene and metal. Table III summarizes the calculated binding energies between metals and both pristine and defective graphene. The binding energies for ideal Au-G, Pt-G, and Pd-G contact are −0.03 eV, −0.04 eV, and −0.08 eV per C atom, respectively, agreeing well with the previous report.[31] The binding energies for the top and bridge site defected contacts are −0.06 eV and −0.05 eV per C atom for Au-G contact, −0.06 eV and −0.05 eV per C atom for Pt-G contact, and −0.15 eV and −0.12 eV per C atom for Pd-G contact. These results indicate that the enhanced M-G interaction can be achieved by introducing defects into graphene.

TABLE III. The binding energy of ideal M-G contacts and defected M-G contacts with different graphene vacancy sites.

	Binding energy (eV/C atom)		
	Top	Bridge	Ideal
Au	−0.06	−0.06	−0.03
Pt	−0.12	−0.07	−0.04
Pd	−0.15	−0.12	−0.08

The transport properties of M-G contact with single C vacancy are studied. We choose the model of the M-G (M = Au, Pt, and Pd) contact with H-terminated graphene end and introduce a single C vacancy on top of a metal atom. The width of the slab model in the transverse direction is enlarged to 9.84 Å to minimize the interaction between neighboring periodic vacancies. The calculated I-V curves in Fig. 6(b) show a considerably increased conductance for Au-G contact with a point defect. These results imply the additional transport channels are introduced between the weakly interacting metal Au and graphene. The dangling bonds near the single carbon vacancy strongly hybridize with Au, which increases the overlap of the interfacial wavefunction for an enhanced charge injection. The I-V curves of the Pt-G (and Pd-G) contacts with and without point defects are quantitatively similar. As chemical bonds are already formed at the graphene edge of the ideal Pt(or Pd)-G contact, the increased binding due to point defects would lead to limited improvement of the transport property. The isosurface of the electrostatic potential in Fig. 6(c) clearly shows the effective transport channels at the single vacancy region. These results suggest that defects can effectively enhance the bonding between graphene and weakly interacting metals and thus increase the contact conductance. As defects are easily formed at realistic metal-graphene contacts,[25] the enhancement of the electronic transport properties by the presence of defects in graphene should be highlighted and even utilized for the optimization of the electrical contacts.

IV. CONCLUSIONS

We report a systematic study on the modulation of the contact resistance between metals (Au, Ag, Pt, Cu, Ni, and Pd) and graphene by altering the termination of the graphene edge, contact area, and defects in graphene, based on a first-principles non-equilibrium Green's function investigation. Besides the role of metal electrodes, the nature of graphene ends, contact areas, and point defects in contacted graphene substantially affects the structural configuration and electronic transport properties of metal-graphene side contact. For the most weakly interacting metals, Au and Ag, graphene ends with increased chemical reactivity and the presence of point defects in graphene can enhance the metal-graphene bonding, leading to reduced contact resistance. The stronger the metals interact with the pristine graphene, the less this enhancement effect is. These six metals are therefore classified into three groups (Au and Ag, Pt and Cu, and Ni and Pd) according to their intrinsic bonding with graphene and the corresponding degree of contact resistance modulation by the studied influencing factors. Our study gives insight of the impact of atomistic details to the electronic transport properties of M-G contacts. It is a good guidance for the optimization of contact resistances in the atomic scale in graphene-based electronic devices.

ACKNOWLEDGMENTS

This work was supported by the National Natural Science Foundation of China (Grant Nos. 11004068, 51302094, and 51101064), the National Basic Research Program of China (Grant Nos. 2011CB606401 and 2013CB934800). The authors acknowledge the Thousand Young Talents Plan, New Century Excellent Talents (NCET) and the Program for Changjiang Scholars and Innovative Research Team (PCSIRT) in University. K.C. is supported by Nano Material Technology Development Program through the National Research Foundation of Korea (NRF) funded by the Ministry of Science, ICT and Future Planning (2012M3A7B4049888). The authors also acknowledge the Texas Advanced Computing Center (TACC) at The University of Texas at Austin (http://www.tacc.utexas.edu) for providing grid resources that have contributed to the research results reported within this paper.

[1]K. S. Novoselov, Rev. Mod. Phys. **83**, 837 (2011).
[2]A. K. Geim, Rev. Mod. Phys. **83**, 851 (2011).
[3]P. Avouris, Nano Lett. **10**, 4285 (2010).
[4]R. M. Westervelt, Science **320**, 324 (2008).
[5]Q. Ran, M. Gao, X. Guan, Y. Wang, and Z. Yu, Appl. Phys. Lett. **94**, 103511 (2009).
[6]Y. Matsuda, W. Deng, and W. A. Goddard, J. Phys. Chem. C **114**, 17845 (2010).
[7]Y. Matsuda, W. Deng, and W. A. Goddard, J. Phys. Chem. C **111**, 11113 (2007).
[8]H. Liu, H. Kondo, and T. Ohno, Phys. Rev. B **86**, 155434 (2012).
[9]E. Watanabe, A. Conwill, D. Tsuya, and Y. Koide, Diamond Relat. Mater. **24**, 171 (2012).
[10]C. E. Malec and D. Davidovicacute, Phys. Rev. B **84**, 33407 (2011).
[11]R. S. Sundaram, M. Steiner, H. Chiu, M. Engel, A. A. Bol, R. Krupke, M. Burghard, K. Kern, and P. Avouris, Nano Lett. **11**, 3833 (2011).
[12]B. Huang, M. Zhang, Y. Wang, and J. Woo, Appl. Phys. Lett. **99**, 032107 (2011).
[13]V. K. Nagareddy, I. P. Nikitina, D. K. Gaskill, J. L. Tedesco, R. L. Myers-Ward, C. R. Eddy, J. P. Goss, N. G. Wright, and A. B. Horsfall, Appl. Phys. Lett. **99**, 73506 (2011).
[14]K. Nagashio, T. Nishimura, K. Kita, and A. Toriumi, Appl. Phys. Lett. **97**, 143514 (2010).
[15]J. A. Robinson, M. LaBella, M. Zhu, M. Hollander, R. Kasarda, Z. Hughes, K. Trumbull, R. Cavalero, and D. Snyder, Appl. Phys. Lett. **98**, 53103 (2011).
[16]C. E. Malec, B. Elkus, and D. Davidović, Solid State Commun. **151**, 1791 (2011).
[17]K. Stokbro, M. Engelund, and A. Blom, Phys. Rev. B **85**, 165442 (2012).
[18]H. M. Liu, H. Kondo, and T. Ohno, J. Chem. Phys. **139**, 074703 (2013).
[19]M. M. Ugeda, D. Fernandez-Torre, I. Brihuega, P. Pou, A. J. Martinez-Galera, R. Perez, and J. M. Gomez-Rodrıguez, Phys. Rev. Lett. **107**, 116803 (2011).
[20]S. Barraza-Lopez, M. Vanević, M. Kindermann, and M. Chou, Phys. Rev. Lett. **104**, 076807 (2010).
[21]J. Maassen, W. Ji, and H. Guo, Nano Lett. **11**, 151 (2011).
[22]J. Maassen, W. Ji, and H. Guo, Appl. Phys. Lett. **97**, 142105 (2010).
[23]Ç. Ö. Girit, J. C. Meyer, R. Erni, M. D. Rossell, C. Kisielowski, L. Yang, C.-H. Park, M. F. Crommie, M. L. Cohen, S. G. Louie, and A. Zettl, Science **323**, 1705 (2009).
[24]L. Xie, L. Jiao, and H. Dai, J. Am. Chem. Soc. **132**, 14751 (2010).
[25]C. Gong, S. McDonnell, X. Qin, A. Angelica, H. Dong, Y. J. Chabal, K. Cho, and R. M. Wallace, ACS Nano **8**, 642–649 (2014).
[26]G. Kresse and J. Furthmüller, Comput. Mater. Sci. **6**, 15 (1996).
[27]J. Taylor, H. Guo, and J. Wang, Phys. Rev. B **63**, 245407 (2001).
[28]J. M. Soler, E. Artacho, J. D. Gale, A. García, J. Junquera, P. Ordejón, and D. Sánchez-Portal, J. Phys.: Condens. Matter **14**, 2745 (2002).
[29]G. Schull, T. Frederiksen, M. Brandbyge, and R. Berndt, Phys. Rev. Lett. **103**, 206803 (2009).
[30]R. Avriller and T. Frederiksen, Phys. Rev. B **86**, 155411 (2012).
[31]C. Gong, G. Lee, B. Shan, E. M. Vogel, R. M. Wallace, and K. Cho, J. Appl. Phys. **108**, 123711 (2010).
[32]Q. J. Wang and J. G. Che, Phys. Rev. Lett. **103**, 66802 (2009).
[33]J. T. Smith, A. D. Franklin, D. B. Farmer, and C. D. Dimitrakopoulos, ACS Nano **7**, 3661 (2013).
[34]B. Shan and K. Cho, Phys. Rev. B **70**, 233405 (2004).
[35]S. Nakanishi and M. Tsukada, Phys. Rev. Lett. **87**, 126801 (2001).
[36]Y. F. Wang, J. Kröger, R. Berndt, H. Vázquez, M. Brandbyge, and M. Paulsson, Phys. Rev. Lett. **104**, 176802 (2010).
[37]M. Paulsson and M. Brandbyge, Phys. Rev. B **76**, 115117 (2007).
[38]L. Wang, X. Y. Zhang, H. L. W. Chan, F. Yan, and F. Ding, J. Am. Chem. Soc. **135**, 4476 (2013).
[39]See supplementary material at http://dx.doi.org/10.1063/1.4876738 for details about the contact configurations and transport properties of the related metals-graphene contact.